On the Deconvolution of Measured Curves with Measured Apparatus Functions and the Information Content of Curves

H. Hühnermann and N. Menzel *

Fachbereich Physik der Philipps-Universität Marburg, D-3550 Marburg

Z. Naturforsch. **34a**, 399–404 (1979); received December 8, 1978

A general problem in natural science is the analysis of experimental curves, which are quite often distorted due to the measuring devices. However, in some cases the apparatus function can be measured separately so that one can hope to restore the original curve by means of a suited mathematical procedure. Based on experimental examples taken from atomic physics and without complicated mathematical formalism, we show possibilities and limitations of the deconvolution of measured curves with measured apparatus functions. The choice of the Fourier transformation algorithm makes it possible to compute the information content of curves quite easily. This may be used to optimize the performance of an experiment.

1. Introduction

Experimentally obtained curves are, in general, smoothed, broadened and distorted due to the measuring devices. In many cases it is possible to measure the apparatus function separately or to compute a theoretical apparatus profile. A deconvolution of the apparatus function from the measured curves should improve the quality of the curve and increase the resolution. However, this deconvolution is limited by spurious fluctuations (noise) in the measured curve. In optical interference spectroscopy one can measure the apparatus function with the help of monochromatic light of a laser with great precision [1] (for earlier measurements and calculations of apparatus functions see [2, 3] and references in [4]). Therefore, optical experiments are a good means to study the possibilities and limitations of deconvolution procedures applied to measured curves (in simple cases the deconvolution has been performed with precalculated tables [5] or electronically [4]).

The intention of this paper is not to reproduce a well known mathematical deconvolution formalism but to show by arbitrarily chosen examples its applicability to physical problems.

2. Experimental Details

The hyperfine structure (hfs) in the cadmium line ^{113}Cd 5s6s $^3S_1$–5s5p $^3P_2$ $\lambda = 508.5$ nm consists of three components, a strong, well resolved one and a smaller doublet with partly overlapping lines where any improvement of resolution is easily recognizable. Figure 1 shows the large peaks at both ends of the experimental curve which are the same hfs-components but measured in adjacent interference orders. The line was excited in a liquid helium or liquid nitrogen cooled hollow cathode discharge. The light of the discharge was preselected by a monochromator and highly resolved with a pressure scanned Fabry-Perot interferometer which is an apparatus commonly used in optical hfs investigations. It consists of two semitransparent highly reflecting mirrors. The optical path

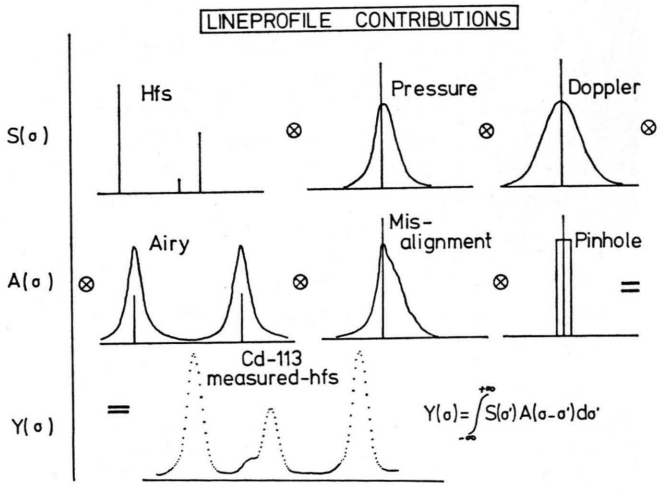

Fig. 1. Main contribution to the line profile of a measured hyperfine structure. The contributions of the source profile $S(\sigma)$ convolved ($\otimes$) with the apparatus function $A(\sigma)$ yield the measured curve $Y(\sigma)$ of the hfs of the ^{113}Cd spectral line $\lambda = 508.5$ nm.

* Now Gesellschaft für Strahlen- und Umweltforschung mbH., D-8042 Neuherberg.

Reprint requests to Prof. Dr. H. Hühnermann. Please order a reprint rather than making your own copy.

0340-4811 / 79 / 0300-0399 $ 01.00/0

between the mirrors is linearly increased by linearly increasing the pressure of a high refractive index gas. The fringe system of the interferometer is projected to an aperture with a pinhole; thus only the light of its central portion is detected by a photomultiplier. During one experimental run the light signals of some 10 interference orders were digitally recorded and later on superposed in order to improve the signal-to-noise ratio. Further details of the line structure, and the measurement and the analysis of the hfs-curves are given in [6].

The monochromatic light of an argon laser ($\lambda = 514.5$ nm) was recorded in the same way as the hfs of the cadmium line. The shape of the recorded laser line is entirely due to the apparatus. From the chosen experimental conditions the line profile contributions shown in Fig. 1 had to be expected. Besides the hfs splitting and the negligible natural line width of the hfs components (Fig. 1, upper left), in a low pressure discharge, despite strong cooling, one is mainly concerned with Doppler-broadening owing to the thermal motion of the light emitting atoms. Broadening effects due to the mutual interaction of the atoms of the gas discharge as resonance broadening, collision broadening etc. are pressure dependent and may therefore be summarized by a pressure broadening contribution. The convolution of these contributions will be referred to as the source profile $S(\sigma)$ of the light source.

The apparatus profile (Fig. 1, middle) consists of the Airyfunction of the ideal Fabry-Perot interferometer and contributions due to mirror defects and misalignments [7]. The scanning aperture (pinhole) can be described by a rectangular function. The convolution of these contributions will be referred to as the apparatus profile $A(\sigma)$.

$S(\sigma)$ as well as $A(\sigma)$ determine the shape of the experimental curve $Y(\sigma)$ via the convolution equation

$$Y(\sigma) = \int_{-\infty}^{+\infty} A(\sigma - \sigma')\, S(\sigma')\, \mathrm{d}\sigma' \tag{1}$$

or in the product notation

$$Y(\sigma) = A(\sigma) \times S(\sigma)\,. \tag{2}$$

In the following we will try to reconstruct $S(\sigma)$ from the measured $Y(\sigma)$ and $A(\sigma)$.

3. Deconvolution

3.1. Fourier Formalism and Fourier Spectra of Measured Curves

The retrieval of the source profile $S(\sigma)$ from the two measured profiles $A(\sigma)$ and $Y(\sigma)$ is easily done in the Fourier transform domain. Let $F(\omega)$ represent the Fourier spectrum (FS) of $F(\sigma)$ [8]:

$$F(\omega) = \int_{-\infty}^{+\infty} F(\sigma)\, e^{-2\pi i \omega \sigma}\, \mathrm{d}\sigma \tag{3}$$

then the convolution (1), (2) is reduced to a simple multiplication

$$Y(\omega) = A(\omega)\, S(\omega)\,. \tag{4}$$

Correspondingly, a deconvolution is performed by a division of the respective FS. An inverse Fourier transformation of $Y(\omega)/A(\omega)$ yields the desired source profile $S(\sigma)$.

The way of proceeding is schematically shown in Figure 2.

The starting point is the Fourier spectrum of the measured hfs pattern. Because of the periodicity of the interferograms and the discrete data sampling, discrete Fourier transformation has to be applied. The nth coefficient of the discrete Fourier-spectrum X_n is defined in analogy to Eq. (3) by

$$X_n = \sum_{k=0}^{N-1} x_k\, e^{-2\pi i n k/N}\,, \quad k, n = 0, \ldots, N-1\,. \tag{5}$$

The FS were computed using the fast Fourier transform algorithm of Cooley and Tukey [9]. In

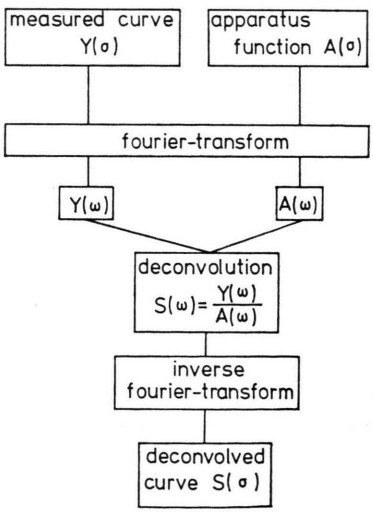

Fig. 2. Steps of a deconvolution procedure using the Fourier transformation formalism.

analogy to Eq. (1) and Eq. (4) the convolution relation is given [10] by

$$y_n = \sum_{k=0}^{N-1} a_{n-k}\, s_k\,, \quad k, n = 0, \ldots, N-1 \qquad (6)$$

or in the Fourier transform domain

$$Y_r = A_r S_r\,. \qquad (7)$$

To illustrate the Fourier analysis of a measured curve, Fig. 3 shows the FS (amplitudes plotted against the discrete spatial frequencies) of a ^{113}Cd hfs-pattern. We appraise as a striking feature of the spectrum that only a small number of coefficients is significantly different from zero and that these coefficients are rapidly decreasing in size with increasing spatial frequency ω. This will be used in 4. to compute the information content of a measured curve. From a certain frequency onwards ($n = 14$) the coefficients are due to the noise always present in measured curves. The noise spectrum, which is in our case more or less "white", hides the signal spectrum completely at high frequencies. Therefore it is obvious that the signal-to-noise ratio in a measured curve will act as a limiting factor for the deconvolution procedure.

3.2. *Deconvolution of Calculated and Measured Curves*

In Fig. 4 the frequency spectrum of a ^{113}Cd curve before and after the deconvolution with a Doppler

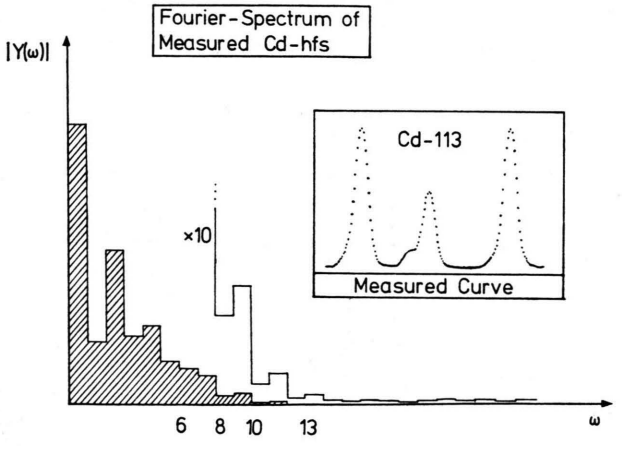

Fig. 3. Discrete Fourier spectrum of the experimental curve shown on the right. The 14th and higher coefficients are mainly due to spurious scatter (noise).

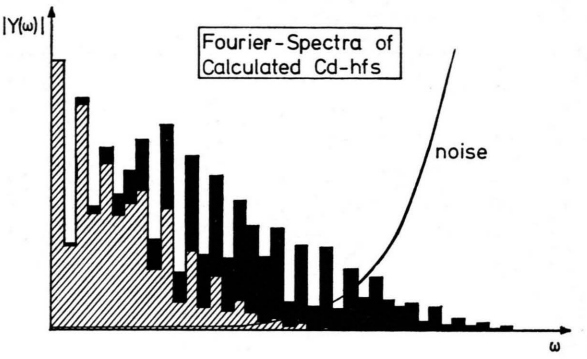

Fig. 4. Deconvolution of a theoretical line profile with an artificial apparatus function. Lower curve: Fourier spectrum of the theoretical line profile (^{113}Cd, but with smaller linewidth as in Figure 3). Upper curve: Fourier spectrum of the deconvolved curve. If one assumes a small frequency independent contribution of noise in the lower curve one gets a noise spectrum in the upper curve as shown.

curve is shown. The calculations according Eqs. (5) and (7) were applied to theoretical line profiles free of noise. As the linewidth decreases due to the deconvolution, the FS of the deconvolved curve necessarily consists of more and larger coefficients. Obviously a deconvolution acts upon the FS like a multiplication with a factor rapidly increasing with frequency. To demonstrate the influence of noise on the deconvolution, a small fraction of white noise is now assumed. By the same factor by which the Fourier coefficients of the signal were multiplied, any noise contribution is amplified, too. In a measured curve the noise amplitudes stay finite up to high frequencies. Therefore, in a deconvolved curve a rapid growth of the noise amplitudes with frequency has to be expected (Fig. 4), and one can easily see that the FC of the signal, which were hidden in the noise before a deconvolution, will remain hidden in the noise spectrum after the performance of the deconvolution operation.

After these considerations the outcome of the deconvolution operation performed with an experimental hfs-curve and a measured apparatus function is not surprising. It is shown in Fig. 5, picture "A + B". Due to the noise the hfs is hardly visible.

In the Fourier spectrum of the deconvolved curve a signal part A and a noise part B is well separated in frequency and it should be easy to find a low pass filter function which cuts off the high frequency noise. However, in some Fourier

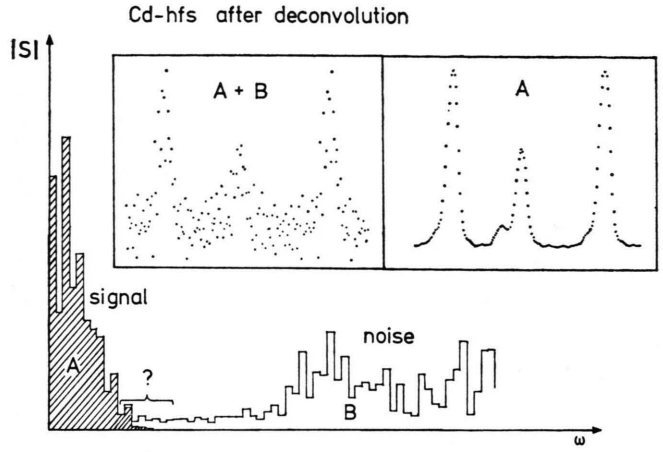

Fig. 5. Deconvolution of the experimental line profile with the experimental apparatus profile and its Fourier spectrum. A + B: Inverse Fourier transform of the deconvolved spectrum. A: Inverse Fourier transform of the deconvolved and filtered spectrum.

coefficients the signal and noise contributions are of comparable magnitude. In this region of the frequency scale, marked with a "?" in Fig. 5, the particular shape of the filter function is of eminent importance. Simple rectangular filtering leads to erroneous results because the sharp cut-off introduces oscillations in the deconvolved curve. Figure 6 gives some examples of the truncation error introduced by a rectangular filtering of the Fourier spectrum of the experimental curve shown in Figure 3. Better suited low-pass filters have functions smoothly varying with the frequency and depending on the signal to noise ratio. But even then the filtering distorts the deconvolved curve and gives rise to spurious oscillations (see Figure 5, A). The amplitude and frequency of these oscillations are very sensitive to the quality of the filter functions applied.

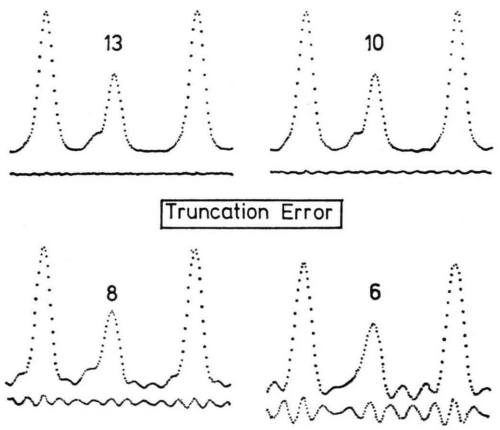

Fig. 6. Truncation error. Distortion of the ^{113}Cd curve, Fig. 3, if its Fourier spectrum is filtered with a rectangular function (low-pass filter). The cut-off Fourier coefficients are given. Below the difference of experimental minus filtered curve.

3.3. Conclusion

The considerations in 3.1 and the result of an actual deconvolution in 3.2 show that it is not possible to improve the measured curves considerably by deconvolution techniques. An increase of resolution is necessarily connected with a decrease of the signal-to-noise ratio. The information content of the deconvolved curve is never greater than that of the original one.

Nevertheless the deconvolution procedure can be very useful. It allows for instance to eliminate asymmetries in the line shape. In an experiment an asymmetry was brought in intentionally by a deadjustment of the interferometer. This asymmetry should be mirrored in the hfs pattern. The deconvolved hfs pattern shown in Fig. 7 shows a somewhat smaller linewidth and, accordingly, an improved resolution of the small hfs component.

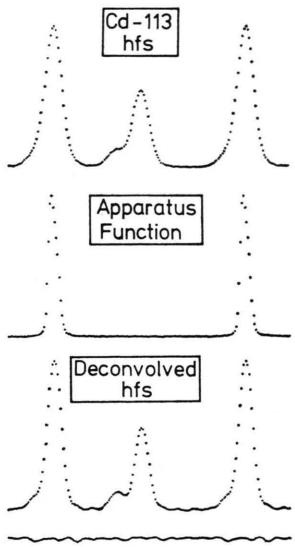

Fig. 7. Deconvolution with an asymmetric apparatus function. The deconvolved (lower) curve has been fitted assuming the residual lineshape to be purely symmetric and of thermal origin. The difference fitted minus deconvolved curve shows the truncation error. Traces of isotopic impurities (^{112}Cd) are visible in the left wing of the large component of the lower curve.

Furthermore, some traces of isotopic impurities (mainly ^{112}Cd) are now visible in the left wing of the large component.

By means of a computer program briefly described in [12] the deconvolved curve had been analyzed with respect to the Doppler width and the Airy- and pinhole contributions of the apparatus function. As expected the shape of the hfs components could be completely described by a Doppler profile and was free of asymmetries *.

The difference of the deconvolved curve and the optimally fitted calculated one shows again the inevitable oscillations (Fig. 7 at the very bottom). Its main contribution is due to the 14th FC which due to noise remained undetermined in the FS of the measured curve.

As a conclusion we may say that the great advantage of this deconvolution method is to produce line profiles free of asymmetries caused by the apparatus. The reduction of the line width is relatively unimportant and absolutely linked with the improvement of the signal-to-noise ratio in the measured curve.

4. Computation of the Information Content of Experimental and Theoretical Curves

The FS of the ^{113}Cd curve (Fig. 3) indicates how to compute the information content of a measured curve. To describe the hfs, $N=13$ complex FC are necessary, that is, only these few coefficients carry information.

Y_n be the nth FC. It can be represented as a point in the plain of complex numbers. However, due to the noise its location is uncertain within a circle of the area $A=\pi Y^2_{\text{noise}}$ with Y^2_{noise} being the average of $|Y_n|^2$, $n>N$, provided the noise spectrum is frequency-independent. Therefore it is not necessary to calculate Y_n, $n<N$, with arbitrary accuracy. It is sufficient to give its value with a relative accuracy of $\pi {Y_n}^2/\pi Y^2_{\text{noise}}$. To do this one needs

$$i_n = \text{ld}\,({Y_n}^2/Y^2_{\text{noise}}) \tag{8}$$

*bi*nary digi*ts* which means that the information content of the nth FC amounts to i_n *bits*. The information content I of the whole curve is given by

$$I=\sum_1^N i_n\,. \tag{9}$$

* Pressure effects play no important rôle.

The sum has to be carried out only over the N relevant coefficients as the information content of the other coefficients is zero. The information content of the ^{113}Cd curve of Fig. 3 thus calculated turned out to be 182 bit.

The Fourier analysis and the calculation of the information content of measured curves may have two applications. As we have seen, the information content of a measured curve is relatively small so that a few hundred binary numbers are sufficient to store the whole curve in the memory of a computer or on magnetic tape or on punched cards etc. (the normal Hollerith card has memory of 960 bit). Storage of the significant FC is a convenient way to save storage allocation.

More important for experimentalists is the second application: The information content of a measured curve depends on the signal-to-noise ratio, that is on the run-time and the strength of the signal, on the linewidth (narrow lines require many FC for their description) and on the number of resolved components. Figure 8 shows four experimental hfs curves published in recent years by the authors in which these values are widely different. Below each curve the noise is plotted in a four times enlarged scale. The noise has been determined by subtracting the measured curve from the one calculated from the significant FC. The Cd curve was obtained from

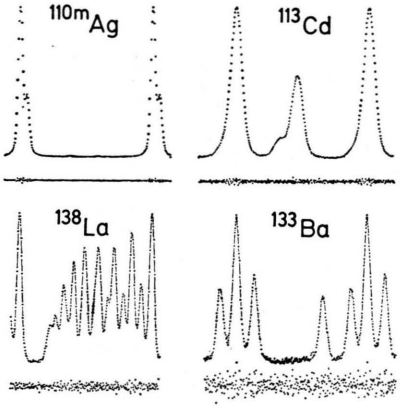

Fig. 8. Normalized experimental curves with differently large relative linewidth, different number of resolved components and different amount of noise, plotted in an enlarged scale 1 : 4, and its information content I, the number of relevant Fourier coefficients N, and the rms noise $\bar{n}$.

^{110m}Ag, $N=38$, $I=549$ bit, $\bar{n}=0.37\cdot10^{-3}$;
^{113}Cd, $N=16$, $I=188$ bit, $\bar{n}=1.8\cdot10^{-3}$;
^{138}La, $N=34$, $I=334$ bit, $\bar{n}=3.8\cdot10^{-3}$;
^{133}Ba, $N=19$, $I=163$ bit, $\bar{n}=10.7\cdot10^{-3}$.

the same experimental data as the previously discussed one. The only difference is the higher number of points (256 instead of 128) used in the superposition. Therefore the signal-to-noise ratio is worse, the whole information remains however approximately the same (187 bit instead of the earlier mentioned 182 bit).

To optimize an experiment one has, in general, to make a compromise between the length of the run-time, signal strength, linewidth, number of resolved components etc. In optical spectroscopy of µg amounts of substances for instance, an increase of the discharge current increases the light intensity but reduces the run-time and increases the linewidth. One can now determine the optimal experimental conditions *in advance* with the help of calculated curves to which an appropriate amount of noise is added. From these curves the information content is calculated as described before. In the case of the ^{113}Cd-hfs, for instance, a reduction of the linewidth of 10% yields the same increase of information of 16 bit as an increase of the measuring time by a factor of 2.5 and a correspondingly better signal-to-noise ratio.

To conclude this section one can say that in all experiments where measured curves can be described by mathematical expressions a Fourier analysis of calculated curves can give valuable hints on a successful performance of an experiment.

This work has been supported by the Bundesminister für Forschung und Technologie.

[1] J. Brochard and R. Vetter, J. Phys. B **7**, 315 (1974).
[2] R. Bacis, Appl. Opt. **10**, 535 (1971).
[3] G. Hernandez, Appl. Opt. **5**, 1745 (1966).
[4] G. T. Best, Appl. Opt. **6**, 287 (1967).
[5] H. G. Kuhn, Atomic Spectra; Longmans, London 1969, p. 416ff.
[6] M. S. W. M. Brimicombe, D. N. Stacey, V. Stacey, H. Hühnermann, and N. Menzel, Proc. Roy. Soc. London A **352**, 141 (1976).
[7] R. Chabbal, J. Rech. Centre Nat. Rech. Sci. Lab. Bellevue **24**, 138 (1953).
[8] R. Bracewell, The Fourier Transform and its Applications. McGraw-Hill, New York 1965.
[9] J. W. Cooley and J. W. Tukey, Math. Comp. **19**, 297 (1965).
[10] W. T. Cochran et al., Proc. IEEE **55**, 1664 (1967).
[11] B. Tatian, J. Opt. Soc. Amer. **61**, 1214 (1971).
[12] H. Hühnermann, J. Physique **28**, C 2-260 (1967).

Verantwortlich für den Inhalt: A. Klemm
Satz und Druck: Konrad Triltsch, Würzburg